Simultaneous Mapping of T_1 and T_2 Using Cardiac Magnetic Resonance Fingerprinting in a Cohort of Healthy Subjects at 1.5T

Jesse I. Hamilton, PhD,[1,2*] Shivani Pahwa, MD,[3] Joseph Adedigba, BS,[3] Samuel Frankel, MD,[3] Gregory O'Connor, MD,[3] Rahul Thomas, MD,[3] Jonathan R. Walker, MD,[3] Ozden Killinc, MD,[3] Wei-Ching Lo, MS,[2] Joshua Batesole, BASc,[3] Seunghee Margevicius, PhD,[4] Mark Griswold, PhD,[2,3] Sanjay Rajagopalan, MD,[3,5] Vikas Gulani, MD, PhD,[1,2,3] and Nicole Seiberlich, PhD[1,2,3]

Background: Cardiac MR fingerprinting (cMRF) is a novel technique for simultaneous T_1 and T_2 mapping.
Purpose: To compare T_1/T_2 measurements, repeatability, and map quality between cMRF and standard mapping techniques in healthy subjects.
Study Type: Prospective.
Population: In all, 58 subjects (ages 18–60).
Field Strength/Sequence: cMRF, modified Look–Locker inversion recovery (MOLLI), and T_2-prepared balanced steady-state free precession (bSSFP) at 1.5T.
Assessment: T_1/T_2 values were measured in 16 myocardial segments at apical, medial, and basal slice positions. Test–retest and intrareader repeatability were assessed for the medial slice. cMRF and conventional mapping sequences were compared using ordinal and two alternative forced choice (2AFC) ratings.
Statistical Tests: Paired *t*-tests, Bland–Altman analyses, intraclass correlation coefficient (ICC), linear regression, one-way analysis of variance (ANOVA), and binomial tests.
Results: Average T_1 measurements were: basal 1007.4±96.5 msec (cMRF), 990.0±45.3 msec (MOLLI); medial 995.0±101.7 msec (cMRF), 995.6±59.7 msec (MOLLI); apical 1006.6±111.2 msec (cMRF); and 981.6±87.6 msec (MOLLI). Average T_2 measurements were: basal 40.9±7.0 msec (cMRF), 46.1±3.5 msec (bSSFP); medial 41.0±6.4 msec (cMRF), 47.4±4.1 msec (bSSFP); apical 43.5±6.7 msec (cMRF), 48.0±4.0 msec (bSSFP). A statistically significant bias (cMRF T_1 larger than MOLLI T_1) was observed in basal (17.4 msec) and apical (25.0 msec) slices. For T_2, a statistically significant bias (cMRF lower than bSSFP) was observed for basal (–5.2 msec), medial (–6.3 msec), and apical (–4.5 msec) slices. Precision was lower for cMRF—the average of the standard deviation measured within each slice was 102 msec for cMRF vs. 61 msec for MOLLI T_1, and 6.4 msec for cMRF vs. 4.0 msec for bSSFP T_2. cMRF and conventional techniques had similar test–retest repeatability as quantified by ICC (0.87 cMRF vs. 0.84 MOLLI for T_1; 0.85 cMRF vs. 0.85 bSSFP for T_2). In the ordinal image quality comparison, cMRF maps scored higher than conventional sequences for both T_1 (all five features) and T_2 (four features).
Data Conclusion: This work reports on myocardial T_1/T_2 measurements in healthy subjects using cMRF and standard mapping sequences. cMRF had slightly lower precision, similar test–retest and intrareader repeatability, and higher scores for map quality.
Evidence Level: 2
Technical Efficacy: Stage 1

J. MAGN. RESON. IMAGING 2020;52:1044–1052.

View this article online at wileyonlinelibrary.com. DOI: 10.1002/jmri.27155

Received Aug 19, 2019, Accepted for publication Mar 13, 2020.

*Address reprint requests to: J.I.H., Medical Science Research Building II, Room 1590B, 1137 Catherine Street, Ann Arbor, MI 48109. E-mail: hamiljes@med.umich.edu

From the [1]Department of Radiology, University of Michigan, Ann Arbor, Michigan, USA; [2]Department of Biomedical Engineering, Case Western Reserve University, Cleveland, Ohio, USA; [3]Department of Radiology, University Hospitals Cleveland Medical Center, Cleveland, Ohio, USA; [4]Department of Population and Quantitative Health Sciences, Case Western Reserve University, Cleveland, Ohio, USA; and [5]Division of Cardiovascular Medicine, University Hospitals Cleveland Medical Center, Cleveland, Ohio, USA

Additional supporting information may be found in the online version of this article

MYOCARDIAL T_1 and T_2 relaxation time mapping is routinely used clinically to aid in the determination of cardiac tissue pathology.[1] Parameter maps depict the values of inherent tissue properties, specifically the time constants for longitudinal relaxation (T_1) and dephasing of transverse magnetization (T_2). Native myocardial T_1, which is measured without administration of gadolinium-based contrast agents, is known to reflect biological characteristics of the myocardium. T_1 values may change in diseases affecting the myocytes and the interstitium. Similarly, changes in native myocardial T_2 have been reported in edema and inflammation.[2,3] Changes in T_1 and T_2 may occur in diseases such as acute coronary syndromes, myocardial infarction, myocarditis, and diffuse fibrosis of various etiologies.[4,5] Similarly, systemic diseases associated with alteration of the extracellular matrix such as amyloidosis, hemosiderosis, and Anderson–Fabry disease cause diffuse changes in T_1.[5,6]

Myocardial T_1 mapping is conventionally performed using sequences including Look–Locker (LL),[7] modified Look–Locker inversion recovery (MOLLI),[8] shortened modified Look-Locker inversion recovery (ShMOLLI),[9] and saturation recovery single-shot acquisition (SASHA).[10] Myocardial T_2 maps may be acquired using fast spin echo,[11,12] balanced steady-state free precession (bSSFP), and gradient spin echo (GRASE) sequences.[13] Recently, techniques have been introduced for joint T_1 and T_2 mapping, including saturation-pulse prepared heart-rate independent inversion-recovery (SAPPHIRE) and other methods.[14–16] However, many of these conventional mapping sequences require the collection of multiple source images with different T_1 and T_2 contrast weightings. The source images are acquired over multiple heartbeats at different timepoints that are assumed to follow an exponential recovery or decay model. Some techniques are prone to errors in the parametric maps if the subject has a rapid or variable heart rhythm, since the measured signals will deviate from their expected exponential timecourses. Moreover, maps collected on different scanners with different hardware performance, pulse sequence timings, or reconstruction software are often inconsistent. Experts recommend collecting normative T_1 mapping data on each magnetic resonance imaging (MRI) scanner before using native T_1 values to characterize pathology.[4] These limitations of existing myocardial parameter mapping methods make it challenging to fulfill the ultimate goal of quantitative MRI—complete tissue characterization based on the specific values of a variety of tissue properties.

Magnetic resonance fingerprinting (MRF) is an emerging method that encodes different tissues, which have distinct T_1 and T_2 values, with distinguishable signal timecourses.[17] The MRF signal timecourses are a result of a specially designed pulse sequence where the acquisition settings are continuously varied during the scan. Signal evolutions from a time series of highly accelerated MRF images are matched to a dictionary of signals simulated using the Bloch equations for 1000 T_1 and T_2 combinations. The T_1 and T_2 measurement for a given voxel is found by identifying the dictionary entry that best matches the measured signal evolution. This pattern matching process is repeated for all voxels to generate quantitative T_1 and T_2 maps.

Cardiac MRF (cMRF) is a promising new adaptation of the MRF framework specifically for myocardial T_1 and T_2 mapping.[18] cMRF data are collected within an ECG-triggered acquisition window during a breath-hold to avoid physiological motion. With ECG-triggered techniques, variations in heart rate affect the amount of T_1 and T_2 relaxation that occurs between acquisition windows. Therefore, a new cMRF dictionary must be created after every scan that models the subject's actual cardiac rhythm in the Bloch equation simulation. By explicitly modeling heart rate effects, cMRF has the potential to be more repeatable, accurate, and precise than traditional cardiac mapping methods. Additionally, the dictionary simulation can include corrections for system imperfections, including slice profile effects, imperfect inversions, or T_2 preparation pulses, and B_1^+ inhomogeneities.[19] Including these corrections could potentially improve the reproducibility of T_1 and T_2 measurements across MRI scanner vendors, software platforms, and institutions.

As with any parameter mapping technique, it is necessary to explore measurement ranges in healthy subjects to use as a reference when comparing to pathologies. The first aim of this study was to summarize T_1 and T_2 measurements obtained with cMRF in healthy adult subjects at 1.5T in comparison with standard cardiac parameter mapping techniques (MOLLI for T_1 mapping, and T_2-prepared bSSFP for T_2 mapping). The second aim was to quantify the image quality, robustness, and repeatability of cMRF in relation to the conventional mapping techniques.

Materials and Methods

In this Institutional Review Board (IRB)-approved and HIPAA-compliant study, 58 subjects (26 men and 32 women; ages 18–60 years, mean 26.9±10.6 years; heart rates 58–100 bpm, mean 74.8± 9.9 bpm) were recruited after obtaining written informed consent. Adult subjects who had no known self-reported history of cardiovascular disease were recruited over 8 months.

Scans were performed with a 1.5T scanner (Siemens Aera, Erlangen, Germany) using an 18-channel cardiac coil array and 12 channels from the built-in spine array. All breath-holds were performed in end-expiration, and volume shimming was performed over the heart. T_1 and T_2 maps were acquired from three short-axis slices at apical, medial, and basal levels of the heart using cMRF, MOLLI, and T_2-prepared bSSFP. During the same scan session, a second set of T_1 and T_2 maps were acquired at the medial slice ~20–30 minutes after the first scan, but without repositioning the subject, to assess test–retest repeatability.

cMRF Acquisition Parameters

A cMRF sequence was employed similar to that described by Hamilton, et al.[18] The scan was ECG-triggered with a 255 msec diastolic acquisition window, and data were acquired during a 15-heartbeat breath-hold with a 192 × 192 matrix, 300 mm^2 field of view (FoV),

and $1.6 \times 1.6 \times 8.0$ mm^3 spatial resolution. A fast imaging with steady-state free-precession (FISP) readout was used with an unbalanced gradient moment along the slice-select axis after each TR.[20] Each scan window was preceded by an inversion pulse (TI 21 msec) or a T_2-preparation pulse (echo times of 30, 50, or 80 msec). During the scan window, RF excitations were applied with variable flip angles between 4–25° and a constant relaxation time / echo time (TR/TE) of 5.3/1.4 msec. Sinc-shaped RF pulses were used with a duration of 0.8 msec and time bandwidth product 2. The *k*-space data were acquired using a variable density spiral trajectory with 48 interleaves that rotated by the golden angle every TR. Data were collected in 50 TRs in each heartbeat over a scan duration of 15 heartbeats, which yielded a total of 750 timepoints in the cMRF signal evolutions. The list of flip angles and preparation pulses, as well as the spiral gradient waveform, are available in the Supporting Information (Supporting File S1.xlsx).

After every scan, a cMRF dictionary was generated containing 26,680 signal evolutions with T_1 values between 10–3000 msec and T_2 values between 2–600 msec. Corrections for slice profile effects and imperfect preparation pulse efficiency were modeled in the dictionary.[19] Principal component analysis (PCA) coil compression was performed on the cMRF data to reduce the number of coils to eight virtual channels. Additionally, to reduce computation time, the dictionary was compressed along the time dimension using the singular value decomposition (SVD),[21] where all singular values smaller than 1% of the maximum singular value were truncated. The cMRF data were projected to the same SVD subspace and then gridded using the nonuniform fast Fourier transform (FFT).[22] At each voxel, parameter maps were generated by finding the dictionary entry that maximized the absolute value of the dot product between the measured signal evolution and the compressed dictionary. All cMRF reconstructions were performed in MatLab (MathWorks, Natick, MA, v. R2018b). On average, each dataset required a total of 2.5 minutes for processing (10 sec for coil compression, 1 sec for gridding, 2.2 min for dictionary generation, and 10 sec for pattern matching).

Acquisition Parameters for Conventional Mapping Approaches

For comparison with cMRF, conventional T_1 maps were acquired using MOLLI with a 5(3)3 acquisition pattern (ie, five imaging heartbeats, three recovery heartbeats, and another three imaging heartbeats) and a breath-hold duration of 11 heartbeats. Conventional T_2 maps were collected during a nine-heartbeat breath-hold using a T_2-prepared bSSFP sequence with a 1(3)1(3)1 acquisition pattern with T_2 preparation times of 0, 25, and 55 msec. Both sequences were acquired with a 192×192 matrix for an in-plane resolution of 1.6×1.6mm^2, 8 mm slice thickness, 35° flip angle, 300 mm^2 FoV, 6/8 partial Fourier, and generalized autocalibrating partial parallel acquisition (GRAPPA) acceleration factor of 2 with 24 calibration lines. The conventional mapping sequences are part of the Siemens MyoMaps software, which calculates the T_1 and T_2 maps online at the scanner using nonlinear curve fitting.

ROI Analysis

A radiologist (S.P.) with 8 years of experience manually drew regions of interest (ROIs) on the T_1 and T_2 maps in segments 1–16 of the standardized American Heart Association (AHA) model. Segment 17 was not well visualized with any sequence and was excluded from the analysis. Care was taken when drawing the ROIs to avoid voxels with partial volume artifacts near the epicardial and endocardial borders. The mean and standard deviation in myocardial relaxation times were computed both within each segment and over the entire slice for cMRF, MOLLI, and T_2-prepared bSSFP. To test intra-reader repeatability, the same radiologist drew ROIs a second time for segments 7–12 in a subset of 20 randomly selected datasets.

Image Quality Assessment

To compare the image quality between cMRF and conventional mapping sequences, ordinal and two alternative forced choice (2AFC) comparisons were performed by three blinded radiologists (S.P., R.T., and S.R.). For the ordinal comparison, medial slice maps from cMRF, MOLLI, and T_2-prepared bSSFP for all subject datasets were presented in a random order. The readers were asked to rate five criteria: 1) sharpness of the endocardial border; 2) sharpness of the epicardial border; 3) visibility of the right ventricular wall; 4) absence of artifacts; and 5) overall diagnostic confidence. Ratings were assigned on a 5-point Likert scale, with 1 being the worst rating. For the 2AFC comparison, medial slice T_1 maps from cMRF and MOLLI were presented side-by-side in a random order, and the radiologists were asked to choose one preferred map. The same comparison was performed for the medial slice T_2 maps comparing cMRF and T_2-prepared bSSFP.

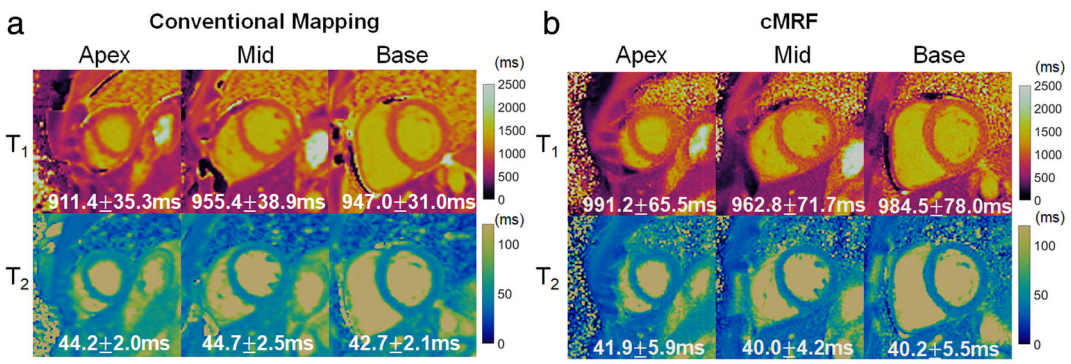

FIGURE 1: Representative maps from three slices in one healthy subject at 1.5T. (a) Maps acquired with conventional techniques (MOLLI and T_2-prepared bSSFP). (b) Maps collected using cMRF. The T_1 and T_2 maps from one slice are collected during one breath-hold.

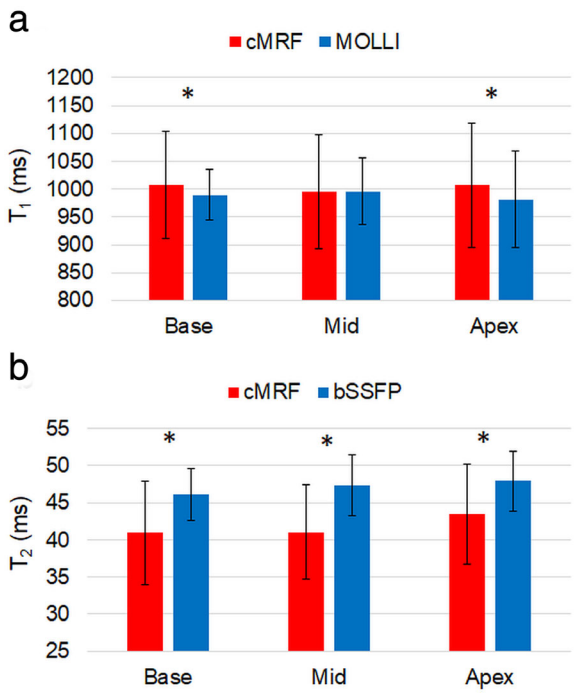

FIGURE 2: T_1 and T_2 measurements in the myocardial wall at basal, medial, and apical slices using cMRF and conventional mapping sequences averaged over 58 subjects. The errors bars indicate the standard deviation. An asterisk (*) indicates that there is a significant difference ($P < 0.05$) between the cMRF and conventional measurements, according to a paired *t*-test.

Statistical Analysis

Differences for every subject between the mean T_1 values measured with cMRF and MOLLI, and the mean T_2 values measured with cMRF and bSSFP, were assessed using a paired *t*-test. These tests were performed using measurements both over the entire slice and within each AHA segment. In addition, the agreement between T_1 and T_2 values collected with cMRF and conventional mapping sequences was assessed using a Bland–Altman analysis.[23] Test–retest repeatability and intrareader repeatability were quantified by calculating the intraclass correlation coefficient (ICC) between the first and second T_1 and T_2 measurements. Additionally, a linear regression was performed and the Spearman correlation was calculated. Data from the ordinal image quality comparison were analyzed using a one-way analysis of variance (ANOVA) to test for significant differences between cMRF and MOLLI T_1 values and cMRF vs. bSSFP T_2 values. The 2AFC image quality data were analyzed using a binomial test. All statistical calculations were performed in R (v. 3.5.1, Vienna, Austria), and a *P*-value less than 0.05 was considered statistically significant.

Results

Representative maps from one subject using cMRF and conventional mapping sequences at three slice positions are shown in Fig. 1. A summary of the myocardial relaxation times measured in basal, medial, and apical slices is given in Fig. 2. The following T_1 measurements were obtained averaged over all subjects: basal 1007.4±96.5 msec (cMRF), 990.0±45.3 msec (MOLLI); medial T_1 995.0±101.7 msec (cMRF), 995.6±59.7 msec (MOLLI); and apical 1006.6±111.2 msec (cMRF), 981.6±87.6 msec (MOLLI). Similarly, the T_2 measurements were: basal 40.9±7.0 msec (cMRF), 46.1±3.5 msec (bSSFP); 41.0±6.4 msec (cMRF), 47.4±4.1 msec (bSSFP); and apical 43.5±6.7 msec (cMRF), 48.0±4.0 msec (bSSFP). Using a paired *t*-test, the differences between cMRF and MOLLI T_1 measurements were significant for the basal

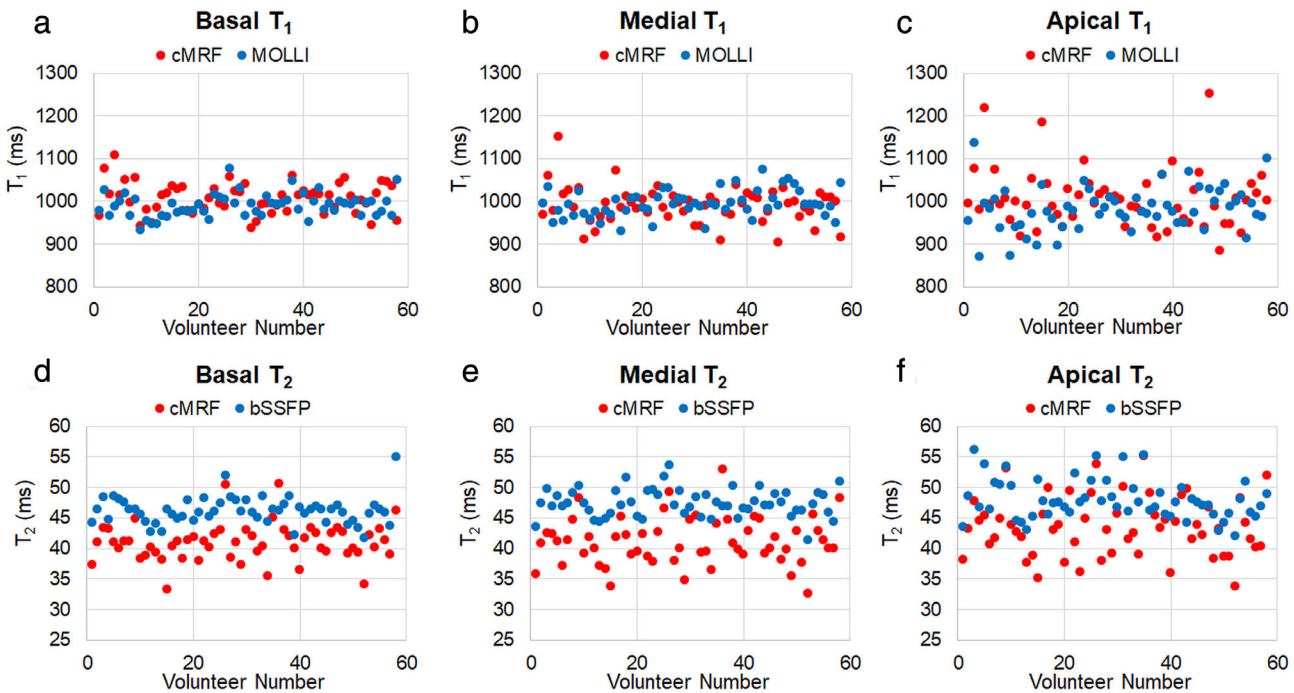

FIGURE 3: T_1 and T_2 measurements collected with cMRF and conventional mapping sequences. Each data point represents the average T_1 and T_2 measured in the myocardial wall in one subject. Results are shown for three slice positions at the base, mid, and apex of the heart.

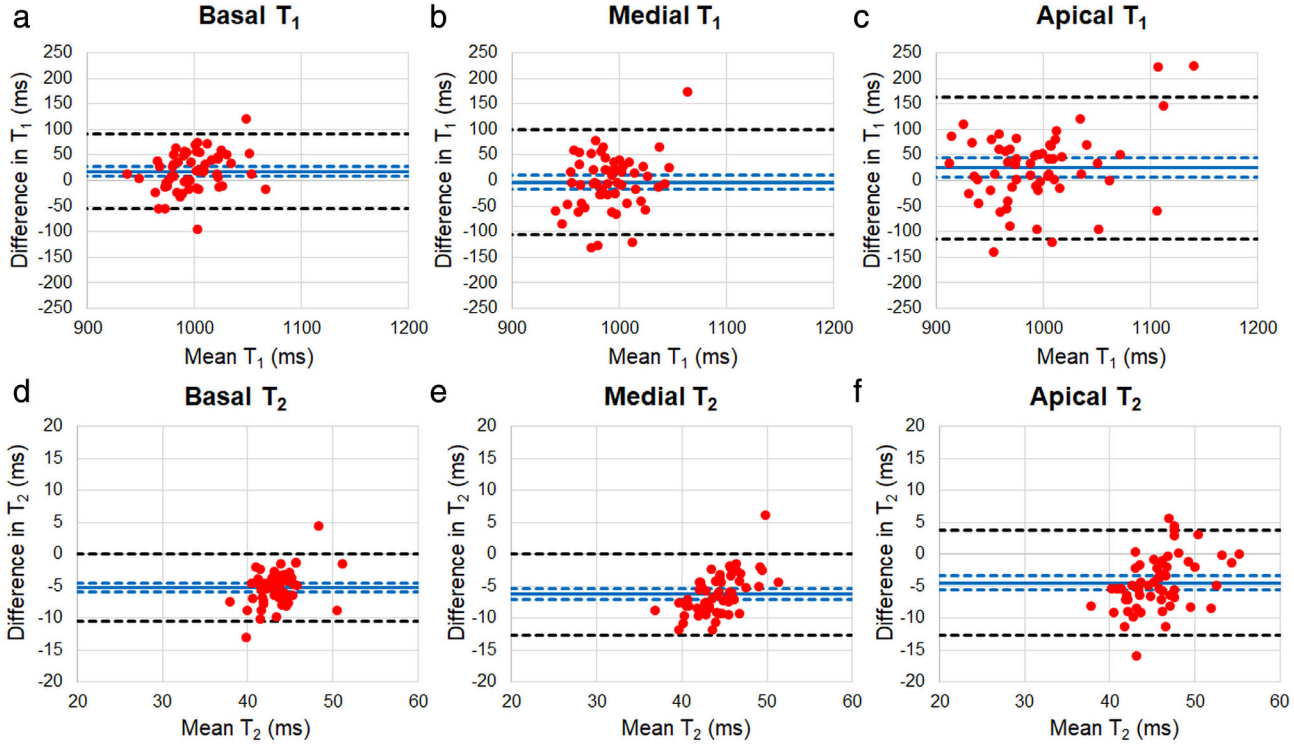

FIGURE 4: Bland–Altman plots comparing cMRF vs. MOLLI T_1 and cMRF vs. bSSFP T_2 measurements in basal, medial, and apical slices. The mean difference (bias) is indicated by the solid blue line, and the 95% confidence interval for the bias is indicated by the two dotted blue lines on either side. The 95% limits of agreement are indicated by the two dotted black lines. The Bland–Altman statistics are summarized in Table 1.

($P < 0.01$) and apical slices ($P = 0.03$), and the differences between cMRF and bSSFP T_2 measurements were significant for all slices ($P < 0.01$). The T_1 and T_2 measurements from each subject are plotted in Fig. 3 for each slice. Figure 4 shows Bland–Altman plots comparing measurements from cMRF and the conventional mapping sequences, and a summary of the Bland–Altman statistics is given in Table 1. The T_1 measurements were overall in good agreement. A positive bias (cMRF T_1 larger than MOLLI T_1) was observed in the basal (17.4 msec) and apical (25.0 msec) slices; these differences are small but statistically significant. For T_2, a statistically significant negative bias (cMRF T_2 lower than bSSFP T_2) was observed for basal (–5.2 msec), medial (–6.3 msec), and apical (–4.5 msec) slices. Figure 5 summarizes the mean and standard deviation of the myocardial T_1 and T_2 measurements grouped by AHA segment. Statistically significant differences ($P < 0.01$) between cMRF and MOLLI T_1 values were seen in basal segments 2–4 and 6; medial segments 8–11; and apical segments 13, 14, and 16. Significant differences ($P < 0.01$) between cMRF and bSSFP T_2 values were observed in all segments except for segment 3.

Test–retest repeatability results for the medial slice T_1 and T_2 are shown in Fig. 6. For T_1, both cMRF and MOLLI had similar Spearman rank correlation coefficients (0.84 vs. 0.81) and ICCs (0.87 vs. 0.84). For T_2, cMRF had a lower Spearman rank correlation coefficient than bSSFP

TABLE 1. Bland–Altman Analysis

Slice	Bias with 95% confidence interval for T_1 (msec)	95% limits of agreement for T_1 (msec)	Bias with 95% confidence interval for T_2 (msec)	95% limits of agreement for T_2 (msec)
Base	17.4 (7.6, 27.3)	(–56.0, 90.9)	–5.2 (–5.9, –4.5)	(–10.5, 0.0)
Mid	–3.6 (–17.5, 10.2)	(–106.8, 99.6)	–6.3 (–7.1, –5.4)	(–12.6, 0.0)
Apex	25.0 (6.4, 43.5)	(–113.4, 163.4)	–4.5 (–5.6, –3.4)	(–12.7, 3.8)

Bland–Altman Statistics Comparing cMRF vs. MOLLI T_1 Values and cMRF vs. bSSFP T_2 Values at Basal, Medial, and Apical Slices (see Fig. 4 for Bland–Altman Plots)

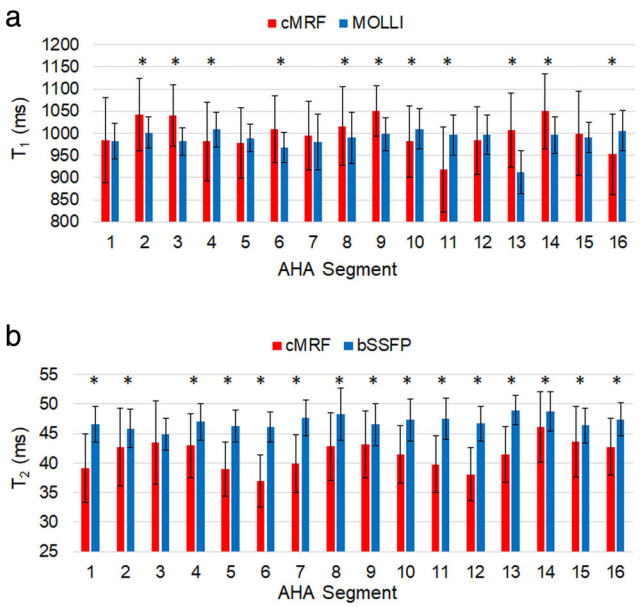

FIGURE 5: Mean T_1 and T_2 values within AHA segments 1–16, averaged over all subjects. The errors bars indicate the standard deviation. An asterisk (*) denotes a statistically significant difference between cMRF and the conventional mapping sequence according to a paired *t*-test ($P < 0.05$).

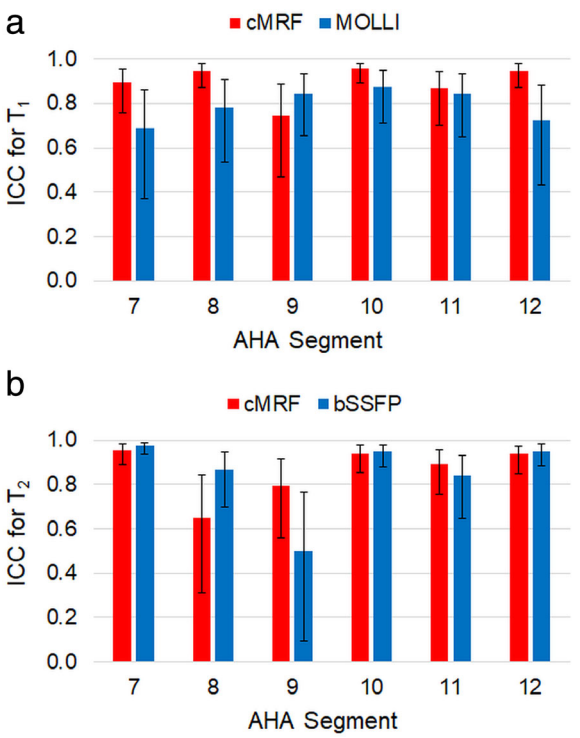

FIGURE 7: Intraclass correlation coefficients (ICCs) calculated from the intrareader repeatability study for T_1 and T_2. The error bars indicate the 95% confidence interval for the ICC estimate.

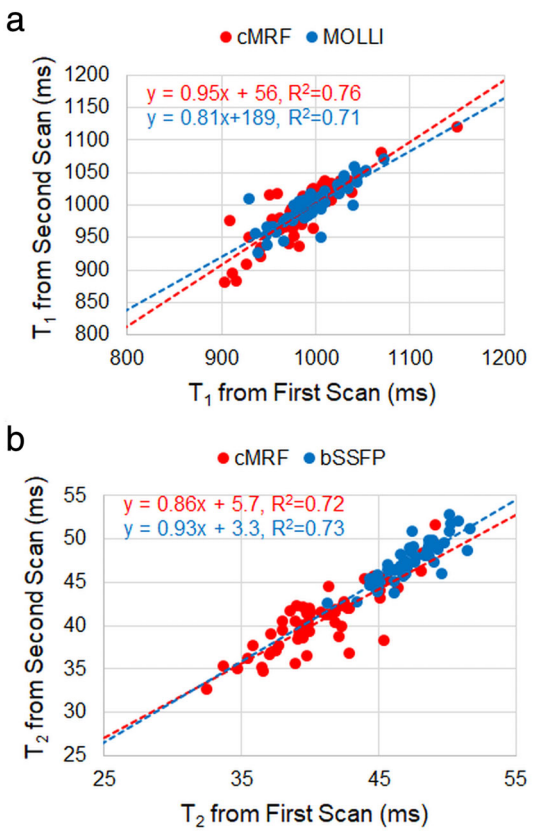

FIGURE 6: Test–retest repeatability results for T_1 and T_2 measured twice with cMRF and conventional methods during the same scan session. The graphs also show the best-fit line for each method and the coefficient of determination (R^2).

(0.79 vs. 0.88), but the two methods yielded similar ICCs (both equal to 0.85). For the intrareader repeatability study, cMRF T_1 values over the medial slice had a higher ICC than MOLLI (0.93 vs. 0.89); for T_2, the ICCs for cMRF and bSSFP were similar (0.94 vs. 0.93). Figure 7 plots the ICCs for intrareader repeatability within each AHA segment. For T_1, the ICCs for cMRF were larger than MOLLI for all segments except for segment 9. For T_2, the ICCs for cMRF were larger than bSSFP for segments 9 and 11; however, the ICCs are approximately equal for segments 7, 10, and 12.

Figure 8 summarizes results from the radiologist ordinal image rating study. For T_1, cMRF was rated higher than MOLLI for all five features. For T_2, cMRF was rated higher than T_2-prepared bSSFP for four out of five features, and both

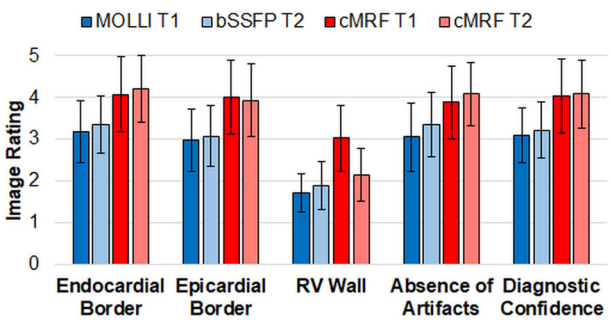

FIGURE 8: Image quality ratings performed by three radiologists averaged over all subject datasets. The error bars indicate the standard deviation.

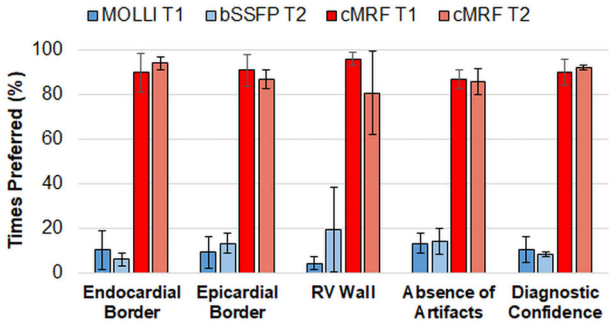

FIGURE 9: Results from the two-alternative forced choice image quality study. The height of each bar reflects the proportion of times that each technique (cMRF, MOLLI, or T_2-prepared bSSFP) was preferred for each feature.

techniques had similarly poor performance for visibility of the right ventricular wall. Figure 9 shows data from the two-alternative forced choice comparison. For both T_1 and T_2, cMRF was preferred over the conventional techniques over 80% of the time for every feature by all radiologists.

Discussion

In this study T_1 and T_2 maps were acquired in a cohort of 58 adult subjects with no known history of cardiovascular disease at 1.5T using both cMRF and conventional cardiac mapping sequences. The intent of this work was to compare the T_1 and T_2 measurements, repeatability, and map quality between cMRF and conventional sequences in healthy subjects. cMRF has previously been demonstrated for rapid multiparametric mapping in myocardial tissue and has several beneficial properties. First, this technique is more efficient than conventional approaches because coregistered T_1 and T_2 maps are acquired simultaneously in one breath-hold. Moreover, the subject's cardiac rhythm is explicitly modeled in the Bloch equation simulation that populates the dictionary. In contrast, conventional mapping techniques usually assume that the magnetization completely recovers between each inversion pulse (for T_1 mapping) or T_2 preparation pulse (for T_2 mapping). This assumption can be violated when subjects have a rapid or variable heart rate, which may cause errors in the quantitative maps.

It is known that MOLLI systematically underestimates T_1 for a variety of reasons, including sensitivity to off-resonance, T_2, heart rate, magnetization transfer, and imperfect inversion efficiency.[24,25] Methods based on saturation recovery, such as SASHA, generally yield more accurate T_1 measurements, although at the expense of lower signal-to-noise ratio (SNR).[26] In this study, the average cMRF T_1 values (999 msec) were similar to those obtained with MOLLI (992 msec), and they agreed with previously published values.[8,9] When each slice was considered separately, cMRF produced slightly higher T_1 values (by 20–30 msec) than MOLLI for apical and basal slices. However, the cMRF T_1 values were still lower than those reported for SASHA (~1150 msec at 1.5T).[27] In this study, the effects of slice profile and imperfect inversion pulse efficiency were modeled in the dictionary. Including these corrections has been shown to increase the myocardial T_1 measured by more than 100 msec at 3T.[19] Thus, other factors, such as magnetization transfer,[28] may be responsible for the suspected underestimation in T_1. Spins bound to macromolecules are not effectively inverted and exchange magnetization with free water molecules, leading to a shorter apparent T_1.

The average myocardial T_2 measured with cMRF (41.3 msec) was significantly lower than that measured with T_2-prepared bSSFP (47.2 msec). Although the reason for this discrepancy is under investigation, it is consistent with previous work using FISP-MRF in the brain, where MRF T_2 values lower than literature values have been reported.[29,30] There are several possible explanations for this difference, including intravoxel dephasing,[31] magnetization transfer, diffusion weighting from the FISP spoiler gradient,[32] and motion sensitivity along the direction of the unbalanced gradient (ie, the slice direction).

Future work will explore ways to improve the precision of cMRF relative to conventional mapping approaches. Over all subjects, the average of the standard deviations measured within each slice was 102 msec for cMRF vs. 61 msec for MOLLI T_1, and 6.4 msec for cMRF vs. 4.0 msec for bSSFP T_2. These differences are partially explained by the SNR of the underlying pulse sequences. The conventional mapping sequences employed a bSSFP readout, which has inherently higher SNR than the FISP readout used for cMRF. Additionally, cMRF employs flip angles less than 25° to minimize errors due to slice profile effects and B_1^+ inhomogeneities; however, these small flip angles further limit the SNR. Better precision could be achieved by a numerical optimization of the cMRF flip angles or preparation pulse timings, which could improve the sensitivity to T_1 and T_2 and also increase SNR.[33] Moreover, an optimal sequence could be tailored for the parameter ranges typically seen in myocardial tissue or designed for optimal sensitivity to certain pathologies. The difference in precision between cMRF and conventional mapping techniques may also be related to differences in postprocessing. The MyoMaps software applies a lowpass filter to the T_1-weighted source images, which may lead to a decrease in the variability in the T_1 and T_2 measurements. Additionally, MyoMaps also applies motion correction to align the individual source images, whereas cMRF does not include these steps.

In this study variations in T_1 and T_2 were observed across different cardiac segments. First, cMRF produced higher T_1 values than MOLLI in anterior, septal, and inferior segments and lower T_1 values than MOLLI in lateral segments. Second, although cMRF consistently yielded lower T_2 values than bSSFP, the difference was more pronounced in lateral segments. Third, cyclic T_1 and T_2 variations were

observed with cMRF, where both T_1 and T_2 were highest in the septal segments and lowest in the lateral segments. Other groups have reported similar trends for T_1, with septal regions having the highest values and lateral regions the lowest.[34,35] This trend was not seen as clearly with the conventional mapping sequences and may be a subject for future investigation. Fourth, with both cMRF and T_2-prepared bSSFP, a small increase in T_2 was observed going from base (40.9 msec for cMRF and 46.1 msec for bSSFP) to apex (43.5 msec for cMRF and 48.0 msec for bSSFP). No variations across slice positions were observed for T_1 (1007 msec for cMRF and 990 msec for MOLLI at the base; and 1007 msec for cMRF and 982 msec for MOLLI at the apex). Other groups have also reported slight increases in T_1 and T_2 going from base to apex.[36]

The test–retest repeatability for cMRF and the conventional methods for T_1 and T_2 were similar according to the ICC values. cMRF had slightly better intrareader repeatability than MOLLI for T_1. For T_2, cMRF had the same or slightly better repeatability than T_2-prepared bSSFP for most segments.

In the image quality rating study, all radiologists consistently ranked cMRF with higher scores than the standard techniques for visibility of the epicardial and endocardial borders, the absence of artifacts, and overall diagnostic confidence. None of the methods achieved good scores for visibility of the right ventricular wall, presumably because the spatial resolution (1.6 mm in-plane) is not sufficient for this application. In the 2AFC experiment, there was a strong preference for cMRF over the conventional maps for every category.

One important factor to consider when translating cMRF to the clinic is reconstruction time. In this study, the dictionary generation time took about 2 minutes on a standard PC running parallelized MatLab Mex code. This time is longer than what was reported previously[18] because of the slice profile and preparation efficiency corrections. Gridding and pattern matching took a total of 20 seconds, which is fast due to the use of dictionary compression.[21] An online reconstruction would further facilitate clinical translation. Preliminary work implementing cMRF in the Gadgetron framework has achieved a reconstruction time less than 2 minutes per slice for an at-the-scanner reconstruction,[37] and machine-learning approaches may also reduce the cMRF reconstruction time.[38,39]

Limitations

There are several limitations to this study. First, as mentioned above, the precision of cMRF was lower than that of the conventional sequences. The precision of cMRF may be improved through numerical optimization of the pulse sequence, residual motion correction, or with novel reconstruction methods. Second, a relatively long scan window (254 msec) was used. This may result in motion artifacts when subjects have rapid heart rates, which may be more commonly encountered in patients rather than healthy subjects. Third, all data were collected on a single scanner. Based on these initial findings, additional reproducibility studies are necessary using cMRF on multiple scanners at different sites and with different scanner vendors. Fourth, this study did not investigate the impact of age, sex, or other confounding variables on T_1 or T_2 measurements, although these effects are known to exist.[40] Fifth, this study only employed cMRF for native T_1 and T_2 mapping. Postcontrast maps were not acquired in these healthy subjects and thus the extracellular volume fraction (ECV) could not be estimated, although the use of cMRF after gadolinium contrast injection is an interesting application for future work. Sixth, this study used a relatively small number of subjects (58) and a limited range of ages (18–60 years). Measurements from additional subjects across a wider range of ages are needed to truly establish reference T_1 and T_2 values for cMRF.

Conclusion

This study reported on the collection of T_1 and T_2 values using cMRF in a cohort of normal subjects. cMRF measurements were compared with those obtained from conventional techniques, specifically MOLLI for T_1 mapping and T_2-prepared bSSFP for T_2 mapping. The test–retest and intrareader repeatability of cMRF compared favorably with the more established techniques. cMRF received overall higher scores in an image quality study performed by two radiologists. The T_1 and T_2 values for cMRF at 1.5T obtained in this study may serve as an initial baseline for future multiscanner, multivendor studies in healthy subjects or patients.

REFERENCES

1. Salerno M, Kramer CM. Advances in parametric mapping with CMR imaging. JACC Cardiovasc Imaging 2013;6:806-822.
2. Bohnen S, Radunski UK, Lund GK, et al. Performance of T1 and T2 mapping cardiovascular magnetic resonance to detect active myocarditis in patients with recent-onset heart failure. Circ Cardiovasc Imaging 2015;8. https://doi.org/10.1161/circimaging.114.003073
3. Radunski UK, Lund GK, Säring D, et al. T1 and T2 mapping cardiovascular magnetic resonance imaging techniques reveal unapparent myocardial injury in patients with myocarditis. Clin Res Cardiol 2017;106: 10-17.
4. Moon JC, Messroghli DR, Kellman P, et al. Myocardial T1 mapping and extracellular volume quantification: A Society for Cardiovascular Magnetic Resonance (SCMR) and CMR Working Group of the European Society of Cardiology consensus statement. J Cardiovasc Magn Reson 2013;15:92.
5. Hamilton-Craig CR, Strudwick MW, Galloway GJ. T1 mapping for myocardial fibrosis by cardiac magnetic resonance relaxometry-a comprehensive technical review. Front Cardiovasc Med 2016;3:49.
6. Messroghli DR, Moon JC, Ferreira VM, et al. Clinical recommendations for cardiovascular magnetic resonance mapping of T1, T2, T2* and extracellular volume: A consensus statement by the Society for Cardiovascular Magnetic Resonance (SCMR) endorsed by the European

Association for Cardiovascular Imagi (EACVI). J Cardiovasc Magn Reson 2017;19:75.

7. Higgins DM, Ridgway JP, Radjenovic A, Sivananthan UM, Smith MA. T1 measurement using a short acquisition period for quantitative cardiac applications. Med Phys 2005;32:1738-1746.
8. Messroghli DR, Radjenovic A, Kozerke S, Higgins DM, Sivananthan MU, Ridgway JP. Modified Look-Locker inversion recovery (MOLLI) for high-resolution T1 mapping of the heart. Magn Reson Med 2004;52: 141-146.
9. Piechnik SK, Ferreira VM, Dall'Armellina E, et al. Shortened modified Look-Locker inversion recovery (ShMOLLI) for clinical myocardial T1-mapping at 1.5 and 3 T within a 9 heartbeat breath-hold. J Cardiovasc Magn Reson 2010;12:69.
10. Chow K, Flewitt JA, Green JD, Pagano JJ, Friedrich MG, Thompson RB. Saturation recovery single-shot acquisition (SASHA) for myocardial T1 mapping. Magn Reson Med 2014;71:2082-2095.
11. Giri S, Chung Y-C, Merchant A, et al. T2 quantification for improved detection of myocardial edema. J Cardiovasc Magn Reson 2009;11:56.
12. de Roquefeuil M, Vuissoz P-A, Escanyé J-M, Felblinger J. Effect of physiological heart rate variability on quantitative T2 measurement with ECG-gated fast spin echo (FSE) sequence and its retrospective correction. Magn Reson Imaging 2013;31:1559-1566.
13. Sprinkart AM, Luetkens JA, Träber F, et al. Gradient spin echo (GraSE) imaging for fast myocardial T2 mapping. J Cardiovasc Magn Reson 2015;17:12.
14. Weingartner S, Akcakaya M, Berg S, Kissinger KV, Manning WJ, Nezafat R. Improved 3D late gadolinium enhancement MRI for patients with arrhythmia or heart rate variability. J Cardiovasc Magn Reson 2013;15:225-226.
15. Akçakaya M, Weingärtner S, Basha TA, Roujol S, Bellm S, Nezafat R. Joint myocardial T1 and T2 mapping using a combination of saturation recovery and T2-preparation. Magn Reson Med 2016;76:888-896.
16. Christodoulou AG, Shaw JL, Nguyen C, et al. Magnetic resonance multitasking for motion-resolved quantitative cardiovascular imaging. Nat Biomed Eng 2018;2:215-226.
17. Ma D, Gulani V, Seiberlich N, et al. Magnetic resonance fingerprinting. Nature 2013;495:187-192.
18. Hamilton JI, Jiang Y, Chen Y, et al. MR fingerprinting for rapid quantification of myocardial T1, T2, and proton spin density. Magn Reson Med 2017;77:1446-1458.
19. Hamilton JI, Jiang Y, Ma D, et al. Investigating and reducing the effects of confounding factors for robust T1 and T2 mapping with cardiac MR fingerprinting. Magn Reson Imaging 2018;53:40-51.
20. Jiang Y, Ma D, Seiberlich N, Gulani V, Griswold MA. MR fingerprinting using fast imaging with steady state precession (FISP) with spiral readout. Magn Reson Med 2015;74:1621-1631.
21. McGivney DF, Pierre E, Ma D, et al. SVD compression for magnetic resonance fingerprinting in the time domain. IEEE Trans Med Imaging 2014;33:2311-2322.
22. Fessler J, Sutton B. Nonuniform fast Fourier transforms using min-max interpolation. IEEE Trans Signal Process 2003;51:560-574.
23. Bland JM, Altman DG. Statistical methods for assessing agreement between two methods of clinical measurement. Lancet 1986;1: 307-310.
24. Kellman P, Hansen MS. T1-mapping in the heart: Accuracy and precision. J Cardiovasc Magn Reson 2014;16:2.
25. Kellman P, Herzka DA, Hansen MS. Adiabatic inversion pulses for myocardial T1 mapping. Magn Reson Med 2014;71:1428-1434.
26. Roujol S, Weingärtner S, Foppa M, et al. Accuracy, precision, and reproducibility of four T1 mapping sequences: A head-to-head comparison of MOLLI, ShMOLLI, SASHA, and SAPPHIRE. Radiology 2014; 272:683-689.
27. Chow K, Yang Y, Shaw P, Kramer CM, Salerno M. Robust free-breathing SASHA T1 mapping with high-contrast image registration. J Cardiovasc Magn Reson 2016;18:47.
28. Robson MD, Piechnik SK, Tunnicliffe EM, Neubauer S. T1 measurements in the human myocardium: The effects of magnetization transfer on the SASHA and MOLLI sequences. Magn Reson Med 2013;70: 664-670.
29. Ma D, Coppo S, Chen Y, et al. Slice profile and B_1 corrections in 2D magnetic resonance fingerprinting. Magn Reson Med 2017;78: 1781-1789.
30. Ma D, Jiang Y, Chen Y, et al. Fast 3D magnetic resonance fingerprinting for a whole-brain coverage. Magn Reson Med 2018;79:2190-2197.
31. Assländer J, Glaser SJ, Hennig J. Pseudo steady-state free precession for MR-fingerprinting. Magn Reson Med 2017;77:1151-1161.
32. Kobayashi Y, Terada Y. Diffusion-weighting caused by spoiler gradients in the fast imaging with steady-state precession sequence may lead to inaccurate T2 measurements in MR fingerprinting. Magn Reson Med Sci 2019;18:96-104.
33. Sommer K, Amthor T, Doneva M, Koken P, Meineke J, Börnert P. Towards predicting the encoding capability of MR fingerprinting sequences. Magn Reson Imaging 2017;41:7-14.
34. Rauhalammi S, Carrick D, Mangion K, et al. 27 regional variations in myocardial T1 relaxation times in healthy adults at 1.5 and 3.0 Tesla. Heart 2015;101:A15.
35. Kim MY, Cho SJ, Choe YH, Kim HJ, Kim SM, Lee S-C. Myocardial T1 mapping in asymptomatic subjects: Variations according to left ventricular segments and correlation with cardiovascular risk factors. J Cardiovasc Magn Reson 2016;18(Suppl 1):119.
36. von Knobelsdorff-Brenkenhoff F, Prothmann M, Dieringer MA, et al. Myocardial T1 and T2 mapping at 3 T: Reference values, influencing factors and implications. J Cardiovasc Magn Reson 2013;15:1-11.
37. Ahad J, Lo W-C, Hamilton JI, Franson D, Jiang Y, Seiberlich N: Implementation of cardiac MRF in gadgetron for online reconstruction. In: Proc. 26th Annu. Meeting ISMRM. Paris, France; 2018, p. 4789.
38. Cohen O, Zhu B, Rosen MS. MR fingerprinting Deep RecOnstruction NEtwork (DRONE). Magn Reson Med 2018;80:885-894.
39. Hamilton JI, Currey D, Griswold M, Seiberlich N. A neural network for rapid generation of cardiac MR fingerprinting dictionaries with arbitrary heart rhythms. In: Proc 26th Annu Meet ISMRM; 2019, p. 2421.
40. Rauhalammi SMO, Mangion K, Barrientos PH, et al. Native myocardial longitudinal (T1) relaxation time: Regional, age, and sex associations in the healthy adult heart. J Magn Reson Imaging 2016;44:541-548.